

Deep Learning Framework for Liver Tumor Segmentation

Khushi Gupta¹, Shrey Aggarwal², Avinash Jha³, Aamir Habib⁴, Jayant Jagtap⁵, Shrikrishna Kolhar^{6,*}, Shrutu Patil⁷, Ketan Kotecha⁸, Tanupriya Choudhury^{9,10}

^{1,2,3,4} Department of Electronics and Telecommunication, Symbiosis Institute of Technology, Symbiosis International (Deemed University), Lavale, Pune, 412115, Maharashtra, India

^{5,6} Department of Artificial Intelligence and Machine Learning, Symbiosis Institute of Technology, Symbiosis International (Deemed University), Lavale, Pune, 412115, Maharashtra, India

^{7,8} Symbiosis Centre for Applied Artificial Intelligence, Symbiosis Institute of Technology, Symbiosis International (Deemed University), Pune, 412115, Maharashtra, India

⁹ CSE Dept., Graphic Era (Deemed to be University), Dehradun, Uttarakhand, 248002, India

¹⁰ CSE Dept., Symbiosis Institute of Technology, Symbiosis International (Deemed University), Pune, 412115, Maharashtra, India

Abstract

INTRODUCTION: Segregating hepatic tumors from the liver in computed tomography (CT) scans is vital in hepatic surgery planning. Extracting liver tumors in CT images is complex due to the low contrast between the malignant and healthy tissues and the hazy boundaries in CT images. Moreover, manually detecting hepatic tumors from CT images is complicated, time-consuming, and needs clinical expertise.

OBJECTIVES: An automated liver and hepatic malignancies segmentation is essential to improve surgery planning, therapy, and follow-up evaluation. Therefore, this study demonstrates the creation of an intuitive approach for segmenting tumors from the liver in CT scans.

METHODS: The proposed framework uses residual UNet (ResUNet) architecture and local region-based segmentation. The algorithm begins by segmenting the liver, followed by malignancies within the liver envelope. First, ResUNet trained on labeled CT images predicts the coarse liver pixels. Further, the region-level segmentation helps determine the tumor and improves the overall segmentation map. The model is tested on a public 3D-IRCADb dataset.

RESULTS: Two metrics, namely dice coefficient and volumetric overlap error (VOE), were used to evaluate the performance of the proposed method. ResUNet model achieved dice of 0.97 and 0.96 in segmenting liver and tumor, respectively. The value of VOE is also reduced to 1.90 and 0.615 for liver and tumor segmentation.

CONCLUSION: The proposed ResUNet model performs better than existing methods in the literature. Since the proposed model is built using U-Net, the model ensures quality and precise dimensions of the output.

Keywords: Computed Tomography (CT) Scans, Deep Learning, Liver Tumor Segmentation, ResUNet, Support Vector Machine, Deep Neural Network

Received on 23 December 2023, accepted on 20 March 2024, published on 27 March 2024

Copyright © 2024 K. Gupta *et al.*, licensed to EAI. This is an open access article distributed under the terms of the [CC BY-NC-SA 4.0](https://creativecommons.org/licenses/by-nc-sa/4.0/), which permits copying, redistributing, remixing, transformation, and building upon the material in any medium so long as the original work is properly cited.

doi: 10.4108/eetpht.10.5561

* Corresponding author. Email: shrikrishna.kolhar@sitpune.edu.in

1. Introduction

As per the report by the World Health Organization (WHO), of all cancers, liver tumor is the most significant cause of death. Every year, roughly 8 lakh people are diagnosed with liver cancer worldwide, with approximately 7 lakh deaths. According to the American Cancer Society's estimates for

2023, about 41,210 fresh instances of primary liver cancer will be diagnosed in the US, and roughly 29,380 will be deceased [1]. These statistics show that the liver cancer incidence trend is on the rise.

Among several medical imaging procedures, Computed Tomography (CT) imaging is commonly used to segment the liver or to diagnose liver cancer [2]. On the other hand, manual detection of liver tumors from CT scans takes a long

time and is subject to observer variability and expertise. As a result, creating an effective computer-aided diagnosis system (CAD) to aid radiologists in liver cancer detection is essential.

The liver has two lobes, right and left, and is connected to the gallbladder, pancreas, and intestines. Because the liver interacts with so many organs, there are two leading causes of cancer in the liver: first, due to the liver's numerous cells, and second, liver metastases that spread through cancerous cells from other organs.

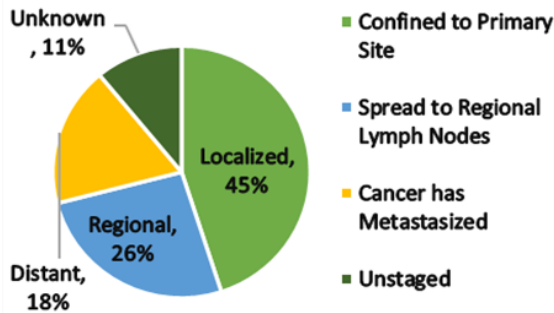


Figure 1. Percent of cases by stages of liver cancer

In medical imaging, automatic liver tumor segmentation is a technique for recognizing, categorizing, and separating the liver from non-liver tissues and malignancies from healthy cells. These methods include training deep-learning models with massive amounts of ground-truth labels of the liver and tumor segmented from medical images by professional radiologists and doctors. The software or a computer-assisted system can include these thoroughly tested and confirmed procedures. Thus, establishing an efficient and precise liver tumor segregation algorithm without clinical experts' intervention will save massive amounts of money, time, and lives [3].

Existing deep learning (DL) segmentation algorithms are broken down into two categories: first, fully convolution network (FCN), which includes U-Net, multi-channel FCN, and VGG-based FCN, and second, 3D-FCN, with 3D convolutions instead of regular 2-D convolutions [4].

The size of cancer in the body at the time of diagnosis, as shown in Figure 1, dictates treatment options and substantially impacts survival time. In general, cancer is said to be localized when it is discovered only in the area of the body where it first appeared, sometimes referred to as stage

1. If the cancer has progressed to another body part, it is classified as regional or remote. The earlier a person's liver and cancer are diagnosed, the better their odds of surviving five years after diagnosis [5]. Local-stage tumors account for 44.6% of liver and intrahepatic bile duct malignancies.

2. Literature survey

Medical imaging and deep learning (DL) have recently been extensively used, and significant growth has been observed in these fields [6]-[8]. Cancer or tumor detection research using medical imaging and DL models with convolution layers has been prevalent. Sharma et al. [9] used random forest (RF), and k-nearest neighbour (k-NN), machine learning (ML) models for prediction of breast cancers. In another study, Khari et al. [10] implemented CNNs to identify brain tumors. Solanki et al. [11] presented a detailed review of the use of various ML algorithms for brain tumor detection and classification.

Any surgical procedure requires tumor segmentation. Accurate and exact tumor location and shape are needed for improved treatment regimens at various stages of liver cancer. This allows for the therapy to be tracked over time. The literature presents multiple methodologies for liver cancer segmentation. Roy et al. [12] proposed an edge detection-based approach for liver cancer nuclei segmentation using histopathological scans. Anter et al. [13] presented a detailed study on liver tumor diagnosis optimization using ML. Another study highlights the use of deep learning in segmenting and classifying liver tumors [14]. Traditional image processing, computer vision, and machine learning approaches classify the features extracted from CT images [15]. These methods extract features such as intensities of pixels, color, texture, size, and shape of tumors from liver CT scans and then employ a classifier method on these features to determine segmented images.

CNN consists of several convolution layers to distinguish high and low-level features from the CT images [16], [17]. The first and foremost step is to develop a CAD system for liver cancer detection [18]; for this purpose, various deep-learning models are helpful. Figure 2 enlists some research methodologies available in the literature. The literature reports the use of statistic shape model (SSM), machine learning (ML) classifiers [19]-[21], clustering, graph-cut, and other semi-automatic liver tumor segmentation models [22]-[24].

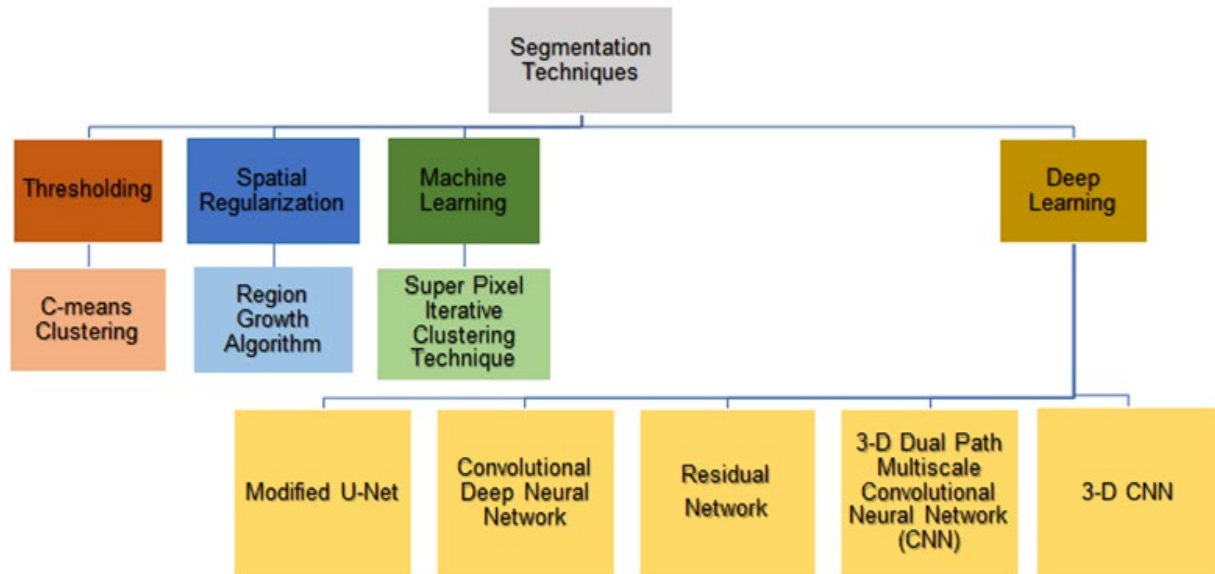


Figure 2. Methodologies for liver cancer segmentation through literature

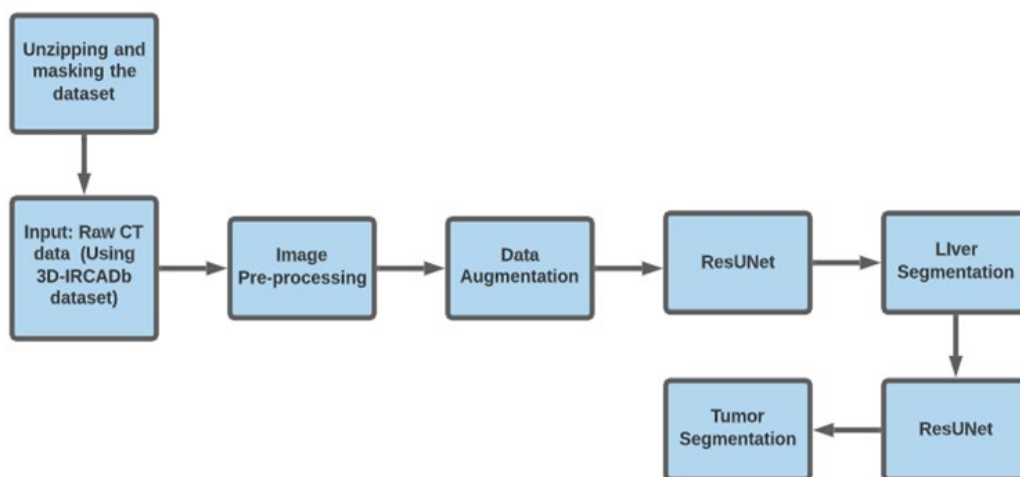


Figure 3. Proposed framework for liver and tumor segmentation

3. Methodology

This paper presents a step-wise DL-based approach for segmenting liver and hepatic tumors from CT scan images. The main contributions of the study are as follows.

- (i) Data augmentation introduces variations in the dataset by employing various data augmentation techniques like rotation, flipping, zooming, cropping, and color changes that increase the image samples in the database.
- (ii) The decrease in the number of kernels at each convolution layer leads to a significant reduction in the training time of the network on the given dataset.

- (iii) The algorithm improves the efficiency of tumor recognition from CT images by alleviating the frames without tumor pixels and keeping frames only with complete information. This helps in reducing the class imbalance between the tumor and background.

Figure 3 depicts the step-wise proposed framework. The steps involved in the framework are as follows.

- (i) Input images in the dataset are raw CT scan images. The input images are normalized and filtered in the pre-processing stage to remove unwanted noise.

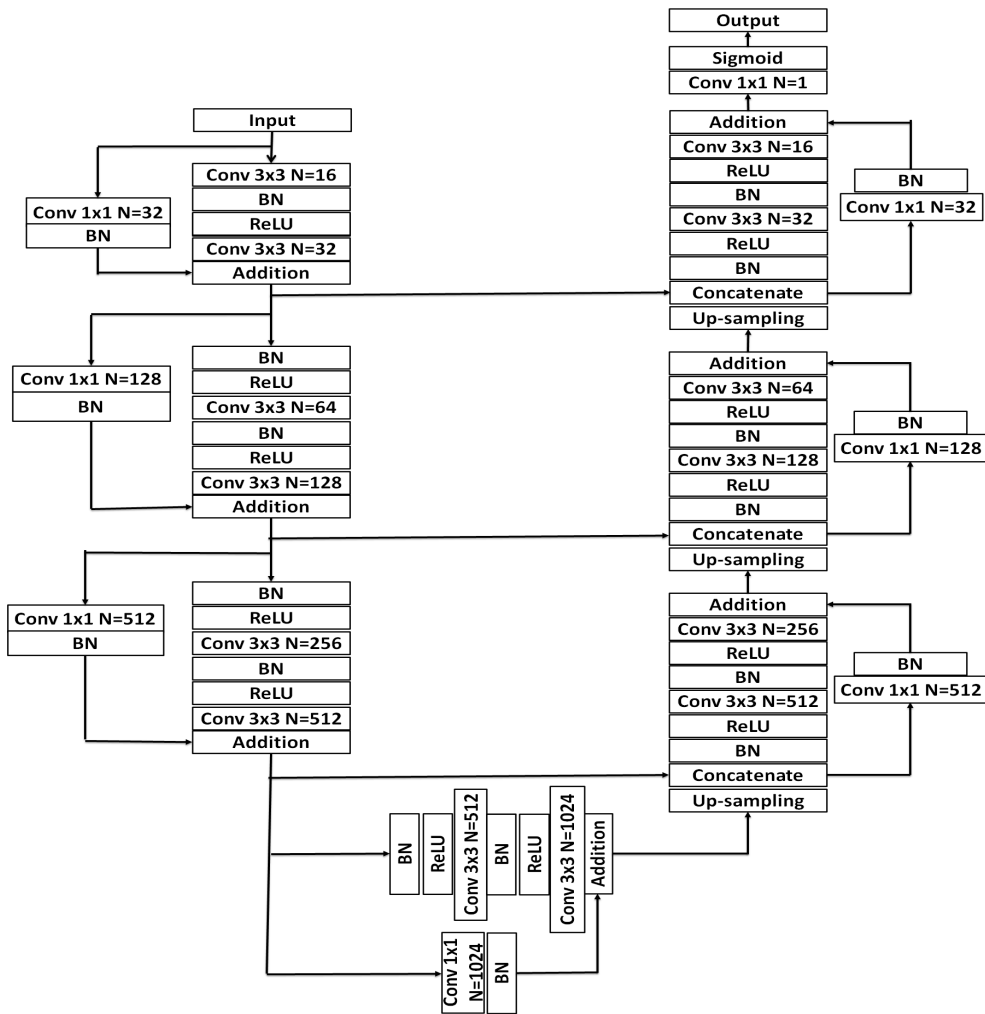


Figure 4. Residual UNet architecture

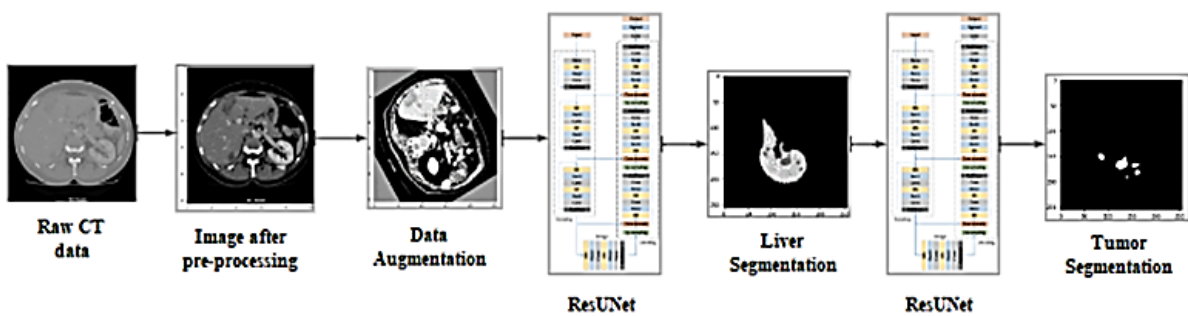


Figure 5. Image flow diagram of the proposed method for liver and tumor segmentation

- (ii) The liver and the malignancies in the liver images are segregated using a DL model called ResUNet.
- (iii) ResUNet architecture consists of a contraction (encoder) and expansion (decoder) path and a bottleneck layer between the contracting (encoder) and expanded (decoder) path, as shown in Figure 4.
- (iv) Encoder and down-sampling: ReLU activation followed by batch normalization (BN) is used in the

encoder path. The encoder determines the semantics of the image to carry out segmentation. These features provide information about the context of the image using convolution layers. Max-pooling helps reduce the size of feature maps, leading to down-sampling. Max-pooling layers follow the convolution layer and ReLU activation functions.

- (v) Bottleneck layer: The layer between the encoder and decoder is the bottleneck layer. The bottleneck layer has two convolution layers and a BN. The bottleneck layer is the layer for maximum abstraction responsible for detecting high-level features in an input image. The bottleneck layer bridges the encoder and decoder path, allowing the network to fuse high-level semantics and detailed spatial information.
- (vi) Decoder and up-sampling: The decoder comprises four layers. In these blocks, the deconvolution or up-convolution layers help restore the size of feature maps and give spatial details about the segmented image. Each layer consists of a stride two up-convolution layers. The clipped features from the encoder are mixed with those from the expanding path.
- (vii) At the last layer, the sigmoid activation function segments the liver and tumor from the background. Figure 5 presents the proposed method in terms of an image flow diagram.

3.1. Training and testing of the binary DNN classifier

- (i) The ResUNet model comprises an input layer, three hidden layers in the contraction and expansion paths, and an output layer.
- (ii) The input layer has 26 nodes, and the output layer has two nodes. The three hidden layers have 20, 30, and 15 nodes, respectively.
- (iii) Each neuron in the network was initialized with random weight and bias
- (iv) The ReLU activation is used in hidden layers for each neuron that triggers the flow of gradients.
- (v) Let X be an input image matrix, W be a weight matrix, and B is biased. Then, each neuron provides output in terms of a matrix. A ReLU activation as $\max(0, Y)$ gives a neuron's result.
- (vi) To prevent overfitting, regularization is useful. Hence, L2 regularization is used by appending $\frac{1}{2} \lambda w^2$ term to each calculated network weight.
- (vii) This paper uses cross-entropy in the binary case as a loss function. Stochastic gradient descent (SGD) optimizer trains the network, and the weights are updated using the backpropagation algorithm.

The training process continues till the error is minimized. The parameters and weights of the trained DNN classifier were saved to predict the network's performance on test data.

3.2. Dataset

The database 3D-IRCADb comprises CT scan images [25] and is manually labeled with different segmented parts by medical experts. The dataset includes 3-D CT scans of the livers of ten female and ten male subjects.

The spacing between the slices is 1.6 to 4.0mm, while the resolution between planes is 0.57 to 0.87 mm. These CT scan images are acquired with the person in the inhaling position. The data is split, so the training set will have ten scans, and validation and test sets will have five scans each. The model is trained on different image sizes. Compared to low-resolution image data, the model performs better on 512×512 resolution images, and segmentation performance is boosted by 2% and 7% for liver and tumors. Down-sampling deteriorates tumor segmentation performance. As a result, the models are trained and tested using 512×512 resolution images, and the accuracy is improved significantly as both datasets have the exact resolution.

4. Results and discussions

The results of the implementation and simulation of the grading and segmentation algorithms are described in this chapter. On a Windows 10 64-bit i5 3.6 GHz processor with 8.0 GB RAM, Python was utilized to run the simulation. For classification, two distinct ML algorithms, SVM and DNN, were employed, and the results were compared. Accuracy (AC), sensitivity (SN), and specificity (SP) were used to test the performance of both pixel classes in the liver and the tumor. To evaluate the quality of the suggested techniques to existing approaches, volumetric overlap error (VOE), dice similarity coefficient (DSC), and valid dice coefficient (VDC) are used.

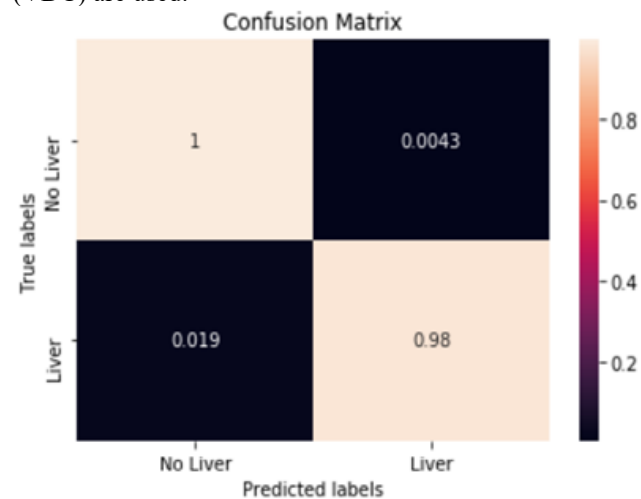


Figure 6. Proposed model confusion matrix for liver

The confusion matrix shown in Figure 6 indicates the classification accuracy and misclassification of image pixels into liver and non-liver regions for ResUNet. Figure 7 shows the confusion matrix for tumor segmentation using ResUNet. The confusion matrices show the ratio of correctly classified pixels out of total number of pixels belonging to a particular class.

The few metrics used to evaluate the model were the DSC, VOE, relative volume difference, and the average symmetric surface distance. The Dice is used to assess the

segmentation results more precisely, with a more significant value suggesting a better outcome. Table 1 shows the results of liver segmentation done through ResUNet, and Table 2 shows the results of our proposed model (ResUNet) for tumor segmentation.

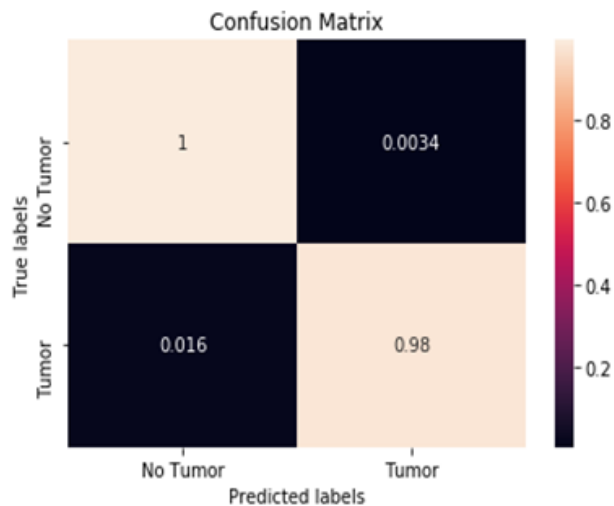


Figure 7. Proposed model confusion matrix for tumor

Table. 1 Experimental results for liver segmentation using ResUNet model

| Epoch | VDC | DSC | AC |
|-------|--------|--------|--------|
| 1 | 0.8934 | 0.8695 | 0.9736 |
| 2 | 0.8432 | 0.9010 | 0.9791 |
| 4 | 0.9054 | 0.9233 | 0.9822 |
| 6 | 0.0209 | 0.9339 | 0.9834 |
| 8 | 0.9396 | 0.9463 | 0.9846 |
| 10 | 0.9170 | 0.9573 | 0.9860 |
| 12 | 0.9172 | 0.9642 | 0.9864 |
| 14 | 0.9550 | 0.9687 | 0.9871 |
| 16 | 0.9740 | 0.9725 | 0.9875 |
| 18 | 0.9762 | 0.9756 | 0.9879 |
| 20 | 0.9780 | 0.9760 | 0.9879 |

The model is tested on a random data sample from the test set and, shown in Figure 8 (a), has a 99.4% and 98.1% true value accuracy. Figure 8 (b) depicts the anticipated liver. Here are the findings of a random sample from the validation data tested on the model. One of the random samples shown in Figure 9 (a) has a 99.8% accuracy and a 93.8% True Value Accuracy and has a dice coefficient of about 95.2%. Figure 9 (b) depicts the anticipated tumor. The two most used techniques for tumor segmentation are SVM and DNN.

Table. 2 Experimental results for tumor segmentation using the ResUNet method

| Epoch | VDC | DSC | AC |
|-------|---------|--------|--------|
| 1 | 0.212 | 0.6386 | 0.9944 |
| 5 | 0.7887 | 0.7620 | 0.9975 |
| 10 | 0.7367 | 0.7800 | 0.9980 |
| 15 | 0.8192 | 0.8130 | 0.9978 |
| 20 | 0.83251 | 0.8270 | 0.9979 |
| 25 | 0.86 | 0.8440 | 0.9982 |
| 30 | 0.8524 | 0.8555 | 0.9984 |
| 35 | 0.7746 | 0.8670 | 0.9985 |
| 40 | 0.7753 | 0.8690 | 0.9984 |
| 45 | 0.8832 | 0.8789 | 0.9987 |
| 50 | 0.8820 | 0.8890 | 0.9986 |

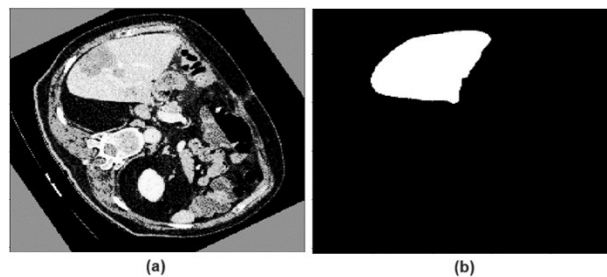


Figure 8. (a) Random sample image taken from the dataset (b) Liver segmented from the sample

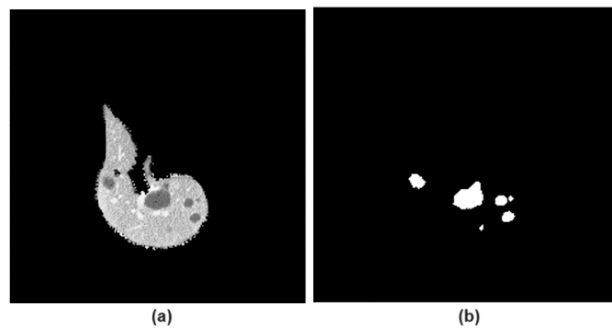


Figure 9. (a) Random sample image taken from the dataset (b) Tumor segmented from the sample.

These two methods were selected to compare the performance of tumor segmentation with the proposed approach. Table 3 presents the results of all three liver and tumor extraction methods in DSC and VOE. Because images with and without tumors were equal, all techniques attained accuracies above 90%. As a result, when the positive and negative examples are uneven, AC is not an acceptable metric for segmentation. Table 3 shows that the ResUNet method achieves a better dice similarity coefficient than other methods.

Table. 3 Evaluation results of different methods for liver and tumor segmentation

| Methods | Tumor segmentation | | Liver segmentation | |
|---------------------|--------------------|-------|--------------------|------|
| | DSC | VOE | DSC | VOE |
| SVM classifier [19] | 96.18 | 0.613 | 96.79 | 2.12 |
| DNN classifier [19] | 95.65 | 0.627 | 97.11 | 1.89 |
| Proposed ResUNet | 96.2 | 0.615 | 97.15 | 1.90 |

5. Conclusion

This paper presents a two-level liver and tumor segmentation approach using the ResUNet model, which needs significantly fewer training parameters than U-Net. The proposed method outperforms two mainly used methods – SVM classifier and DNN classifier. This research uses a public 3D-IRCADb dataset to analyze the performance of the proposed ResUNet model. The methods are tested using performance measures, namely DSC and VOE. The proposed model achieves incremental results in terms of both metrics.

Furthermore, U-net architecture ensures the quality and precise dimensions of the output, similar to the input image. The technique employed in this research can be done without postprocessing to refine the result. The model can be further applied and tested over various datasets. The proposed method implementation, with further improvements, can be used in equivalent medical scenarios. In the future, if adequate processing speed is available, many datasets can be added for analysis. Also, one can use a similar approach for segmentation of other algorithms like lungs, kidneys, brain, etc., and for various medical imaging methods like ultrasound, MRI, etc.

Acknowledgements

The work was supported by the research support fund of Symbiosis International (Deemed University), Pune, India.

References

- [1] Siegel RL, Miller KD, Wagle NS, Jemal A. Cancer statistics, 2023. *CA Cancer J Clin.* 2023;73(1).
- [2] Bilic P, Christ P, Li HB, Vorontsov E, Ben-Cohen A, Kaissis G, Szeskin A, Jacobs C, Mamani GE, Chartrand G, Lohöfer F. The liver tumor segmentation benchmark (lits). *Medical Image Analysis.* 2023 Feb 1;84:102680.
- [3] Rela M, Suryakari NR, Reddy PR. Liver tumor segmentation and classification: A systematic review. *2020 IEEE-HYDCON.* 2020 Sep 11:1-6.
- [4] Huang SY, Hsu WL, Hsu RJ, Liu DW. Fully convolutional network for the semantic segmentation of medical images: A survey. *Diagnostics.* 2022 Nov 11;12(11):2765.
- [5] Galicia-Moreno M, Silva-Gomez JA, Lucano-Landeros S, Santos A, Monroy-Ramirez HC, Armendariz-Borunda J. Liver cancer: therapeutic challenges and the importance of experimental models. *Canadian Journal of Gastroenterology and Hepatology.* 2021 Feb 28;2021.
- [6] Talukdar J, Singh TP, Barman B. Tools and Technologies for Implementing AI Approaches in Healthcare. In *Artificial Intelligence in Healthcare Industry 2023 Jul 2* (pp. 169-178). Singapore: Springer Nature Singapore.
- [7] Sudhakar P, Satapathy SC. A novel skin cancer Detection based transfer learning with optimization algorithm using Dermatology Dataset. *EAI Endorsed Transactions on Pervasive Health and Technology.* 2023 Oct 30;9.
- [8] Agarwal N, Kumar N, Abrol V, Garg Y. Enhancing Image Recognition: Leveraging Machine Learning on Specialized Medical Datasets. *EAI Endorsed Transactions on Pervasive Health and Technology.* 2023 Nov 8;9.
- [9] Sharma S, Aggarwal A, Choudhury T. Breast cancer detection using machine learning algorithms. In *2018 International conference on computational techniques, electronics and mechanical systems (CTEMS) 2018 Dec 21* (pp. 114-118). IEEE.
- [10] Khari S, Gupta D, Chaudhary A, Bhatla R. A Novel Approach to Identify the Brain Tumour Using Convolutional Neural Network. *EAI Endorsed Transactions on Pervasive Health and Technology.* 2023 Nov 8;9.
- [11] Solanki S, Singh UP, Chouhan SS, Jain S. Brain Tumor Detection and Classification using Intelligence Techniques: An Overview. *IEEE Access.* 2023 Feb 6.
- [12] Roy S, Das D, Lal S, Kini J. Novel edge detection method for nuclei segmentation of liver cancer histopathology images. *Journal of Ambient Intelligence and Humanized Computing.* 2023 Jan;14(1):479-96.
- [13] Anter AM, Abualigah L. Deep Federated Machine Learning-Based Optimization Methods for Liver Tumor Diagnosis: A Review. *Archives of Computational Methods in Engineering.* 2023 Jun;30(5):3359-78.
- [14] Saha Roy S, Roy S, Mukherjee P, Halder Roy A. An automated liver tumour segmentation and classification model by deep learning based approaches. *Computer Methods in Biomechanics and Biomedical Engineering: Imaging & Visualization.* 2023 May 4;11(3):638-50.
- [15] Sasirekha N, Anitha R, Vanathi T, Balakrishnan U. Automatic liver tumor segmentation from CT images using random forest algorithm. *The Scientific Temper.* 2023 Sep 27;14(03):696-702.
- [16] Luu MH, Mai HS, Pham XL, Le QA, Le QK, van Walsum T, Le NH, Franklin D, Le VH, Moelker A, Chu DT. Quantification of liver-Lung shunt fraction on 3D SPECT/CT images for selective internal radiation therapy of liver cancer using CNN-based segmentations and non-rigid registration. *Computer Methods and Programs in Biomedicine.* 2023 May 1;233:107453.
- [17] Chen PT, Wu T, Wang P, Chang D, Liu KL, Wu MS, Roth HR, Lee PC, Liao WC, Wang W. Pancreatic cancer detection on CT scans with deep learning: a

- nationwide population-based study. *Radiology*. 2023 Jan;306(1):172-82.
- [18] Chang CC, Chen HH, Chang YC, Yang MY, Lo CM, Ko WC, Lee YF, Liu KL, Chang RF. Computer-aided diagnosis of liver tumors on computed tomography images. *Computer methods and programs in biomedicine*. 2017 Jul 1;145:45-51.
- [19] Song L, Wang H, Wang ZJ. Bridging the gap between 2D and 3D contexts in CT volume for liver and tumor segmentation. *IEEE Journal of Biomedical and Health Informatics*. 2021 Apr 27;25(9):3450-9.
- [20] Barstugan M, Ceylan R, Sivri M, Erdogan H. Automatic liver segmentation in abdomen CT images using SLIC and AdaBoost algorithms. In *Proceedings of the 2018 8th International Conference on Bioscience, Biochemistry and Bioinformatics 2018* Jan 18 (pp. 129-133).
- [21] Muthuswamy J, Kanmani B. Optimization Based Liver Contour Extraction of Abdominal CT Images. *International Journal of Electrical & Computer Engineering* (2088-8708). 2018 Dec 15;8(6).
- [22] Bi L, Kim J, Kumar A, Feng D. Automatic liver lesion detection using cascaded deep residual networks. *arXiv preprint arXiv:1704.02703*. 2017 Apr 10.
- [23] Chlebus G, Schenk A, Moltz JH, van Ginneken B, Hahn HK, Meine H. Automatic liver tumor segmentation in CT with fully convolutional neural networks and object-based postprocessing. *Scientific reports*. 2018 Oct 19;8(1):15497.
- [24] Gruber N, Antholzer S, Jaschke W, Kremser C, Haltmeier M. A joint deep learning approach for automated liver and tumor segmentation. In *2019 13th International conference on Sampling Theory and Applications (SampTA) 2019* Jul 8 (pp. 1-5). IEEE.
- [25] Senthilvelan J, Jamshidi N. A pipeline for automated deep learning liver segmentation (PADLLS) from contrast enhanced CT exams. *Scientific Reports*. 2022 Sep 22;12(1):15794.